Journal of Inorganic and General Chemistry
ZAAC
Zeitschrift für anorganische und allgemeine Chemie
www.zaac.wiley-vch.de
RESEARCH ARTICLE

DOI: 10.1002/zaac.202500154

Complete Series of 1,2-Bis(trihalogenosilyl)benzenes (F, Cl, Br, I): A Platform for Cooperating Lewis-Acidic Sites in Close Quarters

Moritz Schmidt, Niklas H. H. Hürtgen, Alexander Virovets, Hans-Wolfram Lerner, and Matthias Wagner*

Dedicated to Christian Limberg and Franc Meyer on the occasion of their joint 120th birthday

1,2-Bis(trihalogenosilyl)benzenes are versatile synthetic building blocks and represent a unique class of ditopic Lewis acids. Building on the recently reported compound 1,2-$(Cl_3Si)_2C_6H_2Me_2$ ($\mathbf{1^{Cl}}$; Me groups in 4,5-positions), the practical synthetic access to its sixfold fluorinated ($\mathbf{1^{F}}$), brominated ($\mathbf{1^{Br}}$), and iodinated ($\mathbf{1^{I}}$) congeners is disclosed. Compound $\mathbf{1^{F}}$ is obtained via Cl/F exchange on $\mathbf{1^{Cl}}$ using SbF_3 (71%). The synthesis of $\mathbf{1^{Br}}$ involves a [4 + 2]-cycloaddition reaction between $Br_3SiC{\equiv}CSiBr_3$ and 2,3-dimethyl-1,3-butadiene to furnish the corresponding 1,4-cyclohexadiene, which is subsequently dehydrogenated and aromatized using 2,3-dichloro-5,6-dicyano-1,4-benzoquinone (overall 59%). Compound $\mathbf{1^{I}}$ is formed through H/I exchange on 1,2-$(H_3Si)_2C_6H_2Me_2$ with BI_3 (32%). All species $\mathbf{1^{F}}$–$\mathbf{1^{I}}$ are comprehensively characterized by NMR spectroscopy, X-ray crystallography, elemental analysis, and high-resolution mass spectrometry. Moreover, adducts of $\mathbf{1^{F}}$ with either 1 equiv. or 2 equiv. of F^- are shown to form an inverse chelate featuring a Si–(μ-F)–Si′ bridge or a mixed bridging/terminal coordination motif, respectively.

1. Introduction

Organo(halogeno)silanes occupy a central position in both synthetic organic chemistry and materials science, owing to their broad functionalizability and structural diversity.[1] A key reason for their utility lies in the presence of electronegative halogen substituents, which serve a dual purpose: they act as excellent leaving groups in chemical transformations such as hydrolytic condensation and nucleophilic substitution,[2] and they enhance the Lewis acidity of the silicon atoms to which they are attached – a highly desirable asset.[3,4] In the context of this publication, our research focuses on a particular subclass of these compounds, wherein two Si centers are held in close proximity by a rigid 1,2-phenylene bridge (e.g., $\mathbf{1^{Cl}}$; **Figure 1**a). Such a molecular design offers two main benefits. First, it promotes the formation of dual-site Lewis acids with mutually cooperating electron-pair acceptor sites, potentially enhancing their reactivity profile. Second, it enables the development of hybrid polymers that integrate both organic and inorganic components.[5–9] A particularly compelling variant of this approach involves the synthesis of polyhedral silsesquioxanes (POSS).[10,11] Here, the pre-organized geometry provided by the hydrocarbon scaffold in the starting material may impart a degree of structural predictability, guiding the formation of well-defined 3D architectures.

We have synthesized compound $\mathbf{1^{Cl}}$, which had been predicted in the literature to be "almost impossible" to obtain,[12] from readily available $Cl_3SiC{\equiv}CSiCl_3$ and 2,3-dimethyl-1,3-butadiene (DMB) via a [4 + 2]-cycloaddition, followed by oxidative aromatization using 2,3-dichloro-5,6-dicyano-1,4-benzoquinone (DDQ).[13,14] The introduction of two Me substituents in $\mathbf{1^{Cl}}$ is motivated by the practical advantage of using liquid DMB (bp. 68 °C) instead of gaseous 1,3-butadiene (bp. −4.5 °C), as well as by a facilitated analysis of the ^{1}H NMR spectra. Building on this work, we demonstrated that the number of functionalizable Cl substituents in $\mathbf{1^{Cl}}$ can be systematically tuned.[15] In this context, we found that prolonged heating of a cyclic derivatization product of $\mathbf{1^{Cl}}$ leads to the formation of a 1,3-disila-2-oxaindane, accompanied by the release of pinacolone (Figure 1b). The mechanistic details of this transformation confirm the intrinsic value of two cooperating Lewis-acidic Si centers for unlocking novel reactivity.

Herein, we expand the scope of 1,2-bis(trihalogenosilyl) benzenes to encompass the complete series 1,2-$(X_3Si)_2C_6H_2Me_2$ (X = F, Cl, Br, I), with the dual objective of 1) installing leaving groups X of varying reactivities and 2) modulating the Lewis acidities of the two cooperating X_3Si substituents. We then show that 1,2-$(F_3Si)_2C_6H_2Me_2$ is capable of binding up to two F^- ions. Finally, we disclose protocols for the targeted synthesis of 1,2-$(HBr_2Si)_2C_6H_2Me_2$ (**2**) and 1,2-$(H_2BrSi)_2C_6H_2Me_2$ (**3**), and demonstrate that the two remaining Br atoms in compound

M. Schmidt, N. H. H. Hürtgen, A. Virovets, H.-W. Lerner, M. Wagner
Institut für Anorganische und Analytische Chemie, Goethe-Universität Frankfurt am Main, Max-von-Laue-Straße 7, 60438 Frankfurt am Main, Germany
E-mail: matthias.wagner@chemie.uni-frankfurt.de

Supporting information for this article is available on the WWW under https://doi.org/10.1002/zaac.202500154

Journal of Inorganic and General Chemistry
ZAAC
Zeitschrift für anorganische und allgemeine Chemie

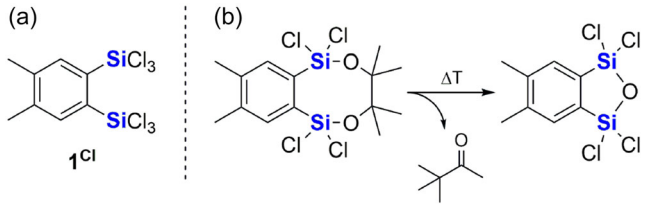

Figure 1. a) Molecular structure of $\mathbf{1}^{Cl}$. b) Thermolysis of the cyclic derivatization product of $\mathbf{1}^{Cl}$ proceeds via a pinacol–pinacolone rearrangement, resulting in a 1,3-disila-2-oxaindane and concomitant release of pinacolone.

3 can be selectively utilized in cyclocondensation reactions, while the Si—H bonds remain untouched.

2. Results and Discussion

Three different access routes to the compounds 1,2-$(X_3Si)_2C_6H_2Me_2$ were evaluated [X = F ($\mathbf{1}^{F}$), Br ($\mathbf{1}^{Br}$), I ($\mathbf{1}^{I}$); **Scheme 1**]: a) halogen exchange on 1,2-$(Cl_3Si)_2C_6H_2Me_2$ ($\mathbf{1}^{Cl}$), b) [4 + 2]-cycloaddition reactions between $X_3SiC{\equiv}CSiX_3$ and DMB, followed by aromatization, and c) conversion of $\mathbf{1}^{Cl}$ to 1,2-$(H_3Si)_2C_6H_2Me_2$ ($\mathbf{1}^{H}$)[16] with subsequent H/X exchange. Here, we focus primarily on the protocols that proved most effective in our hands; additional details are provided in the Supporting Information.

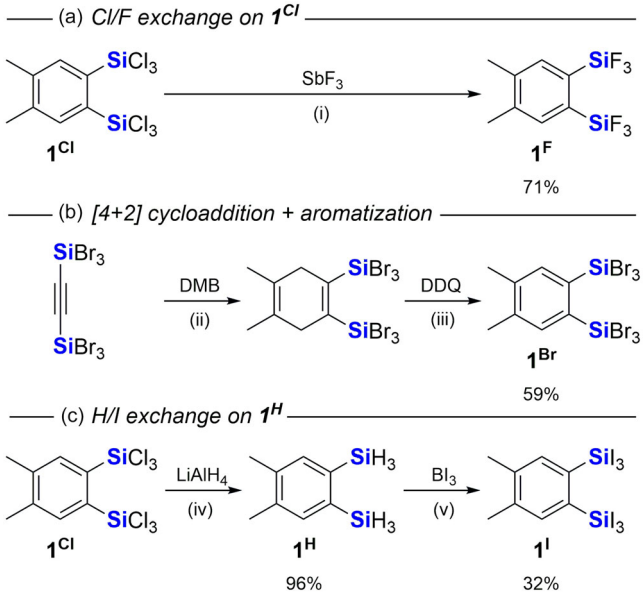

Scheme 1. a) Halogen exchange converts $\mathbf{1}^{Cl}$ to $\mathbf{1}^{F}$, b) [4 + 2]-cycloaddition of $Br_3SiC{\equiv}CSiBr_3$ with 2,3-dimethyl-1,3-butadiene (DMB), followed by oxidative aromatization using 2,3-dichloro-5,6-dicyano-1,4-benzoquinone (DDQ), leads to $\mathbf{1}^{Br}$, and c) reduction of $\mathbf{1}^{Cl}$ with $LiAlH_4$ gives $\mathbf{1}^{H}$; subsequent iodination with BI_3 affords $\mathbf{1}^{I}$. Reagents and conditions: (i) 4.8 equiv. SbF_3, no solvent, room temperature, 14 h; (ii) 1.2 equiv. DMB, C_6H_6, 60 °C, 3 d, sealed glass ampoule; (iii) 2 equiv. DDQ, C_6H_6, room temperature, 14 h; (iv) 3.2 equiv. $LiAlH_4$, Et_2O, room temperature, 14 h; (v) 4 equiv. BI_3, C_6H_6, room temperature, 14 h.

Stirring a solid mixture of $\mathbf{1}^{Cl}$ and SbF_3 under ambient conditions furnished $\mathbf{1}^{F}$ in 71% yield after workup (Scheme 1a). Crystals of $\mathbf{1}^{F}$ suitable for X-ray diffraction were grown by sublimation of the purified product at room temperature under a static vacuum. Compound $\mathbf{1}^{Br}$ is best prepared from $Br_3SiC{\equiv}CSiBr_3$[16] and DMB, which quantitatively afford the corresponding 1,4-cyclohexadiene (Scheme 1b); $\mathbf{1}^{Br}$ is obtained through dehydrogenation of the primary cycloadduct with DDQ (59% overall yield). Finally, $\mathbf{1}^{I}$ was prepared from $\mathbf{1}^{H}$ and BI_3; $\mathbf{1}^{H}$, in turn, is accessible from $\mathbf{1}^{Cl}$ and $LiAlH_4$ (96%; Scheme 1c). Notably, the low yield of $\mathbf{1}^{I}$ (32%) is not due to steric overload, as the actual conversion is higher; however, yield losses inevitably occurred during washing of the crude product, even when cold C_6H_6 was used to minimize the solubility of $\mathbf{1}^{I}$. Crystals of $\mathbf{1}^{Br}$ and $\mathbf{1}^{I}$ were obtained by slow evaporation of their solutions in *n*-hexane and C_6H_6, respectively.

In the course of our search for an efficient synthesis of $\mathbf{1}^{Br}$, we also discovered routes to synthetically useful 1,2-disilylated benzenes bearing well-defined, mixed substitution patterns on the silyl groups: Treatment of $\mathbf{1}^{H}$ with BBr_3 (6 equiv.) in C_6H_6 at room temperature provided 1,2-$(HBr_2Si)_2C_6H_2Me_2$ (**2**) in excellent yields (95%; **Scheme 2**); crystals of **2** suitable for X-ray diffraction formed upon slow evaporation of its *n*-hexane solution (Figure S67, Supporting Information). It is worth emphasizing that, at room temperature, H/Br exchange on $\mathbf{1}^{H}$ stalled at the stage of **2**, even when the reaction was performed in neat BBr_3 (50 equiv.). In contrast, the reaction of $\mathbf{1}^{H}$ with BBr_3 (2.6 equiv.) proceeded to the stage of 1-(Br_3Si)-2-$(HBr_2Si)C_6H_2Me_2$ upon heating to 50 °C for 2 days; extending the reaction time led to substantial decomposition while yielding only trace amounts of $\mathbf{1}^{Br}$ (Figure S2, Supporting Information). The 1,2-$(H_2BrSi)_2$-congener **3** of $\mathbf{1}^{Br}$ and **2** is accessible via bromination of $\mathbf{1}^{H}$ with *N*-bromosuccinimide (NBS; 2 equiv.) at 7 °C under ambient light (Scheme 2). After workup, **3** was obtained with minor contamination by the monobrominated side product 1-(H_2BrSi)-2-$(H_3Si)C_6H_2Me_2$, which had no adverse effect on the use of **3** as starting material in subsequent cyclocondensations (see below).

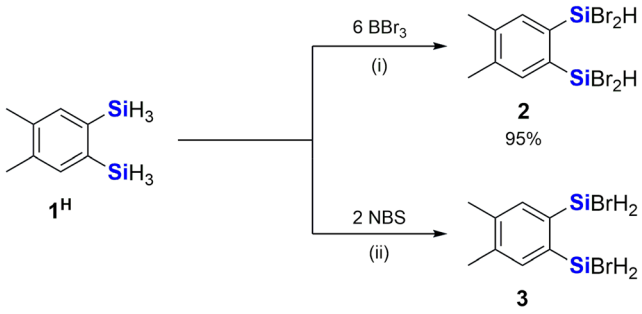

Scheme 2. Two complementary derivatization pathways starting from $\mathbf{1}^{H}$ provide access to compounds **2** and **3** with defined mixed H/Br substitution patterns: reaction of $\mathbf{1}^{H}$ with BBr_3 (upper pathway) affords **2**; reaction of $\mathbf{1}^{H}$ with *N*-bromosuccinimide (NBS) (lower pathway) furnishes the 1,2-$(H_2BrSi)_2$-substituted congener **3**. Reagents and conditions: (i) 6 equiv. BBr_3, C_6H_6, room temperature, 14 h; (ii) 2 equiv. NBS, C_6H_6, 7 °C, ambient light, 14 h.

Journal of Inorganic and General Chemistry
ZAAC
Zeitschrift für anorganische und allgemeine Chemie

The proposed molecular structures of $\mathbf{1^F}$, $\mathbf{1^{Br}}$, and $\mathbf{1^I}$ were confirmed by (heteronuclear) NMR spectroscopy, single-crystal X-ray diffraction (SCXRD), elemental analysis, and high-resolution mass spectrometry. Full details are compiled in the Supporting Information; in the following, only selected features and trends are discussed.[17]

Upon going from F to I, the ^{29}Si NMR resonances of $\mathbf{1^F}$–$\mathbf{1^I}$ follow a nonmonotonic trend [−74.1 ($\mathbf{1^F}$), −2.2 ($\mathbf{1^{Cl}}$),[13] −30.1 ($\mathbf{1^{Br}}$), and −152.6 ppm ($\mathbf{1^I}$); **Table 1**], which qualitatively mirrors the trend observed for the ^{29}Si NMR chemical shift values of $ArSiX_3$ [−72.6 ($PhSiF_3$),[18] 0.6 ($PhSiCl_3$),[18] −35.7 (2,6-$Mes_2C_6H_3SiBr_3$),[19] −175.3 ($MesSiI_3$)[19]].[20] An interesting feature in the ^{19}F NMR spectrum of $\mathbf{1^F}$ is the presence of two satellite signals with quartet multiplicity that accompany the main singlet resonance at −139.6 ppm (**Figures 2**a and S10, Supporting Information). The latter arises from the most abundant isotopologue containing two ^{28}Si atoms [^{28}Si/^{28}Si; $S(^{28}Si) = 0$].[21] All its ^{19}F nuclei are equivalent by symmetry, and no J_{FF} coupling is observed. The second most abundant isotopologue, ^{28}Si/^{29}Si [$S(^{29}Si) = ½$],[21,22] bears two inequivalent $^{28}SiF_3$ and $^{29}SiF_3$ moieties. The satellite signals are thus due to $^1J_{SiF} = 267$ Hz coupling (cf. $PhSiF_3$: $^1J_{SiF} = 267$ Hz[18]), while the quartet multiplicity of each satellite results from (through space)[23] $J_{FF} = 5$ Hz coupling to $^{28}SiF_3$.

Table 1. Trends in ^{29}Si NMR chemical shift values and Si···Si′ interatomic distances for $\mathbf{1^F}$, $\mathbf{1^{Cl}}$, $\mathbf{1^{Br}}$, and $\mathbf{1^I}$. For NMR shifts, increased shielding (upfield shift) is indicated by the wider end of the wedge. For Si···Si′ distances, the wider wedge end denotes larger interatomic distances.

	$\mathbf{1^F}$	$\mathbf{1^{Cl}}$	$\mathbf{1^{Br}}$	$\mathbf{1^I}$
δ(²⁹Si) [ppm]	−74.1	−2.2	−30.1	−152.6
Si···Si′ [Å]	3.54	3.72	3.77	3.87

To investigate the influence of increasing steric repulsion between the silyl groups in the series $\mathbf{1^F}$–$\mathbf{1^I}$, we examined the relative conformation of the two silyl groups in each molecule, along with the Si···Si′ distances, the exocyclic bond angles Si—C—C′ at the silylated C atoms (C, C′) as well as the Si—C—C′—Si′ torsion angles by means of SCXRD (cf. **Figure 3**a, illustrating the molecular structure of $\mathbf{1^F}$ as a representative example). Despite differences in atomic radius and the potential for dispersion interactions among the X substituents, the molecular conformations are highly similar, as evidenced by the overlay of the solid-state structures of $\mathbf{1^F}$–$\mathbf{1^I}$ in Figure 3b.[24] As the atomic radius of the halogen substituent X increases, the Si···Si′ distance also increases continuously from 3.539(1) Å (X = F) to 3.871(3) Å (X = I; Table 1). Concomitantly, analysis of the Si—C—C′ bond angles and Si—C—C′—Si′ torsion angles reveals systematic variations correlated with the steric demands of the silyl substituents (Table S6, Supporting Information). The smallest Si—C—C′ bond angle is observed for parent 1,2-disilylbenzene, 1,2-$(H_3Si)_2C_6H_4$ (123.2[6]°; CSD: XIDXEN[25]). The Si—C—C′ bond angle increases along the series as follows: $\mathbf{1^F}$ (125.5[2]°), $\mathbf{1^{Cl}}$ (128.0[6]°; CSD: PIDMOH[13]), $\mathbf{1^{Br}}$ (128.9[4]°), and $\mathbf{1^I}$ (130.5[5]°).[26] In contrast, the Si—C—C′—Si′ torsion angles remain close to planarity, with absolute values in a narrow range of 0.0(4)°–1.4(1)°, and the benzene moiety exhibits only negligible distortion. This supports the conclusion that $\mathbf{1^F}$–$\mathbf{1^I}$ alleviate steric strain primarily by lateral displacement of the silyl groups within the molecular plane, rather than by twisting them out of plane.

To probe the F^--accepting properties of $\mathbf{1^F}$,[27] the ditopic Lewis acid was treated with the soluble F^- source $[(Me_2N)_3S][F_2SiMe_3]$

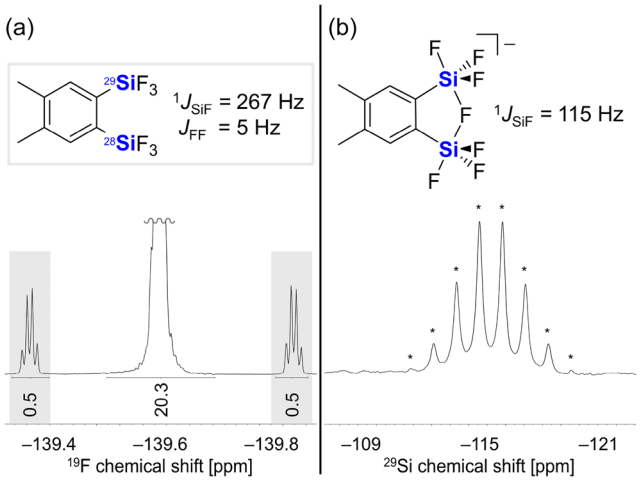

Figure 2. a) Expanded region of the ^{19}F NMR spectrum of $\mathbf{1^F}$ in CD_2Cl_2, showing a main singlet resonance at −139.6 ppm with ^{29}Si satellites featuring a resolved quartet multiplicity ($^1J_{SiF} = 267$ Hz; $J_{FF} = 5$ Hz) and b) expanded region of the $^{29}Si\{^1H\}$ NMR spectrum of $[\mathbf{1^F}{\cdot}F]^-$ in CD_2Cl_2, displaying a well-resolved octet centered at −115.6 ppm ($^1J_{SiF} = 115$ Hz).

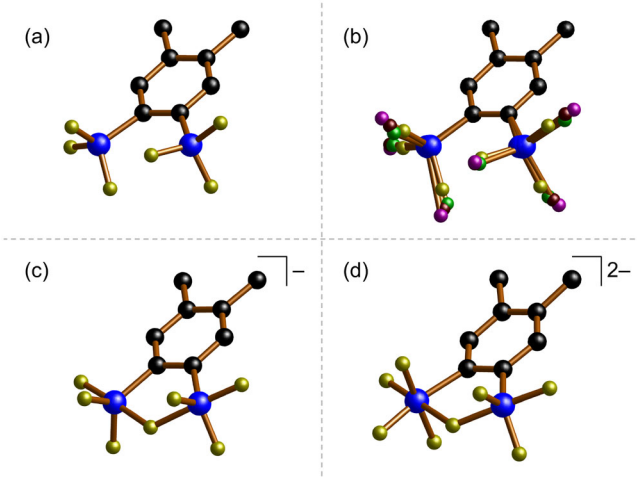

Figure 3. Molecular structures in the crystalline state: a) $\mathbf{1^F}$, b) overlay of $\mathbf{1^F}$, $\mathbf{1^{Cl}}$, $\mathbf{1^{Br}}$, and $\mathbf{1^I}$, c) $[\mathbf{1^F}{\cdot}F]^-$, and d) $[\mathbf{1^F}{\cdot}2F]^{2-}$. H atoms and the $[(Me_2N)_3S]^+$ counterions are omitted for clarity; halogen radii were standardized to that of fluorine to enhance visual comparability. C: black, Si: blue, F: pale yellow, Cl: green, Br: mahogany, I: purple.

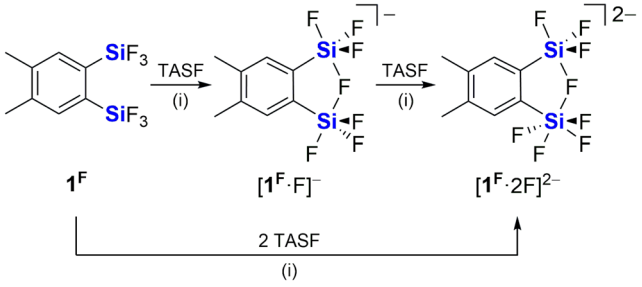

Scheme 3. $\mathbf{1^F}$ reacts with 1 or 2 equiv. of $[(Me_2N)_3S][F_2SiMe_3]$ (TASF) to give $[\mathbf{1^F}\cdot F]^-$ and $[\mathbf{1^F}\cdot 2F]^{2-}$, respectively; $[\mathbf{1^F}\cdot F]^-$ is converted to $[\mathbf{1^F}\cdot 2F]^{2-}$ upon treatment with 1 equiv. of TASF. Conditions: (i) CH_2Cl_2, room temperature, 1 h. For clarity, the $[(Me_2N)_3S]^+$ counterions are omitted.

(TASF) in CD_2Cl_2 or CH_2Cl_2 (**Scheme 3**). At room temperature, the ^{29}Si NMR resonance of $[\mathbf{1^F}\cdot F]^-$ appears as a well-resolved octet at −115.6 ppm, with an average coupling constant of $^1J_{SiF} = 115$ Hz (Figure 2b), which is considerably smaller than that of free $\mathbf{1^F}$ (−74.1 ppm, $^1J_{SiF} = 267$ Hz). The $[\mathbf{1^F}\cdot F]^-$ anion thus represents a rare example of seven F^- ligands undergoing rapid intramolecular exchange between two silicon atoms via Berry pseudorotation.[28] The $[\mathbf{1^F}\cdot 2F]^{2-}$ dianion gives rise to a signal at −139.8 ppm in the ^{29}Si NMR spectrum, with a line shape indicative of an odd-numbered multiplet. Only seven of the expected nine lines have been unambiguously detected, likely due to the two outermost peaks being obscured by noise ($^1J_{SiF} = 107$ Hz; Figure S22, Supporting Information).

In summary (**Table 2**), and in agreement with trends reported in the literature,[28] the ^{29}Si nuclei of $\mathbf{1^F}$, $[\mathbf{1^F}\cdot F]^-$, and $[\mathbf{1^F}\cdot 2F]^{2-}$ become progressively more shielded with increasing coordination number, while the corresponding $^1J_{SiF}$ coupling constants decrease. Next, we monitored the trend in the ^{19}F NMR shift of the mixture $\mathbf{1^F}/n F^-$ as a function of the stoichiometry n (Figure S25, Supporting Information). The sharp ^{19}F resonance of free $\mathbf{1^F}$ at −139.6 ppm ($n = 0$) underwent a downfield shift to −129.6 ppm at $n = 1$ and further to −120.1 ppm at $n = 2$ (Table 2).

Thus, unlike comparable ditopic and potentially chelating silicon-based Lewis acids,[28–30] $\mathbf{1^F}$ is capable of binding not only one, but two F^- ligands to furnish the adducts $[\mathbf{1^F}\cdot F]^-$ and $[\mathbf{1^F}\cdot 2F]^{2-}$, respectively (Scheme 3).[31] Compared to the signal of $\mathbf{1^F}$, the full-width-at-half-maximum (FWHM) values of the shifted resonances increased remarkably, from FWHM ≈2 Hz to ≈43 and ≈75 Hz, respectively. In this context, it is noteworthy that an extremely broad hump centered around −132 ppm was observed at $n = 0.5$, while the resonance of $[\mathbf{1^F}\cdot 2F]^{2-}$ at −120.1 ppm sharpened to a FWHM of ≈9 Hz upon increasing the TASF loading to $n = 3$. All in all, these changes in FWHM values are indicative of dynamic F^--association/dissociation equilibria, which shift toward the adduct species in the presence of excess TASF. In order to gain insight into the molecular structures of the F^- adducts (Figure 3c,d), crystals of $[(Me_2N)_3S][\mathbf{1^F}\cdot F]$ and $[(Me_2N)_3S]_2[\mathbf{1^F}\cdot 2F]$ were grown by gas-phase diffusion of *n*-hexane into CH_2Cl_2 solutions of

Table 2. Trends in heteronuclear NMR chemical shift values, $^1J_{SiF}$ coupling constants, and Si···Si′ interatomic distances for $\mathbf{1^F}$, $[\mathbf{1^F}\cdot F]^-$, and $[\mathbf{1^F}\cdot 2F]^{2-}$. For NMR shifts, increased shielding (upfield shift) is indicated by the wider end of the wedge. For Si···Si′ distances, the wider wedge end corresponds to larger interatomic distances.

	$\mathbf{1^F}$	$[\mathbf{1^F}\cdot F]^-$	$[\mathbf{1^F}\cdot 2F]^{2-}$
$\delta(^{29}Si)$ [ppm]	−74.1	−115.6	−139.8
$\delta(^{19}F)$ [ppm]	−139.6	−129.6	−120.1
$^1J_{SiF}$ [Hz]	267	115	107
$\delta(^{13}C)$ [ppm]	124.3[a]	≈ 140[a, b]	150.7[a]
Si···Si′ [Å]	3.54	3.32	3.37

[a]These ^{13}C NMR shifts refer to the Si-bonded aromatic C atoms (SiC); [b]This SiC signal likely overlaps with the two other aromatic ^{13}C resonances at 139.9 and 139.6 ppm; the shift value is therefore somewhat speculative.

$\mathbf{1^F}$ and TASF in 1:1 and 1:2 ratios, respectively. The monoadduct $[(Me_2N)_3S][\mathbf{1^F}\cdot F]$ crystallizes with two crystallographically independent molecules in the asymmetric unit, both adopting approximate C_{2v} symmetry. In each, a single F^- ion bridges the two Si atoms, which are, in turn, located in a slightly distorted trigonal-bipyramidal environment. The Si—F bonds to the bridging ion are significantly longer [1.815(4)–1.889(5) Å] than those to the terminal F atoms [1.545(4)–1.654(5) Å]. Among the latter, the Si—F_{ax} bonds [1.607(5)–1.654(5) Å] are longer than the Si—F_{eq} bonds [1.545(4)–1.590(3) Å; ax: axial, eq: equatorial]. Insertion of an F^- ligand between the two silyl groups does not push them apart but instead draws them closer together, indicating significant Si—(μ-F) bonding interactions [Si···Si′ = 3.539(1) Å ($\mathbf{1^F}$) vs. 3.310(2), 3.320(3) Å ($[(Me_2N)_3S][\mathbf{1^F}\cdot F]$); Si—($\mu$-F)—Si′ = 125.8(2)°, 127.3(2)°]. The diadduct $[(Me_2N)_3S]_2[\mathbf{1^F}\cdot 2F]$ also contains only one bridging F^- ligand, rather than two; one of the silyl groups adopts a geometry close to trigonal-bipyramidal, the other to octahedral. The two Si—(μ-F) bonds are now distinctly different: the bond involving the pentacoordinate Si atom is shorter than that to the hexacoordinate Si atom [1.774(1) vs. 2.013(1) Å, respectively; Si—(μ-F)—Si′ = 125.6(1)°], and also shorter than the corresponding Si—(μ-F) bonds in the monoadduct $[\mathbf{1^F}\cdot F]^-$. Coordination of a fourth terminal F^- ligand to one Si site has only a minor effect on the Si···Si′ distance in $[\mathbf{1^F}\cdot 2F]^{2-}$ [3.370(1) Å], which remains close to that found in $[\mathbf{1^F}\cdot F]^-$.

The presence of six functionalizable halogen substituents in $\mathbf{1^F}$–$\mathbf{1^I}$ offers broad opportunities for diverse downstream

chemistry. In the context of hydrolytic condensation reactions, however, such monomers tend to form 3D cross-linked, insoluble resins rather than well-defined polymeric or cyclic architectures. This is where compounds of type **2** and **3** come into play, as they feature two distinct types of substituents that can be addressed independently in late-stage derivatizations. In a proof-of-principle experiment, we performed the controlled hydrolysis of **3** in the presence of pyridine as HBr scavenger and obtained the doubly benzannulated, ten-membered $Si_4O_2C_4$ heterocycle **4** in 26% yield after purification by fractional sublimation (**Scheme 4**a).[32] The preservation of all Si—H bonds in **4** is evidenced not only by its solid-state structure (**Figure 4**a; all Si*H* atoms were located in the difference electron-density map and freely refined), but also by a characteristic triplet resonance observed in the ^{29}Si NMR spectrum [$\delta(^{29}Si) = -25.4$; $^1J_{SiH} = 219$ Hz]. A notable outcome of this hydrolysis experiment is that the corresponding 1,3-disila-2-oxaindane **5**, featuring a benzo-fused five-membered Si_2OC_2 ring (Scheme 4a), did not emerge as a major product—if it formed at all.[33] This stands in marked contrast to the result of our attempt to synthesize compound $\mathbf{1^{Br}}$ via sixfold MeO/Br exchange on 1,2-$((MeO)_3Si)_2C_6H_2Me_2$ (**6**) using BBr_3: in that case, C—O-bond cleavage led to the formation of the tetrabrominated 1,3-disila-2-oxaindane **7** (87%), rather than the corresponding dimer with a molecular framework analogous to that of **4** (Scheme 4b, Figure 4b). One reason why **4**- and **7**-type structures can compete, although the latter are entropically favored and avoid the potentially destabilizing effect of a medium-sized ring, might be rooted

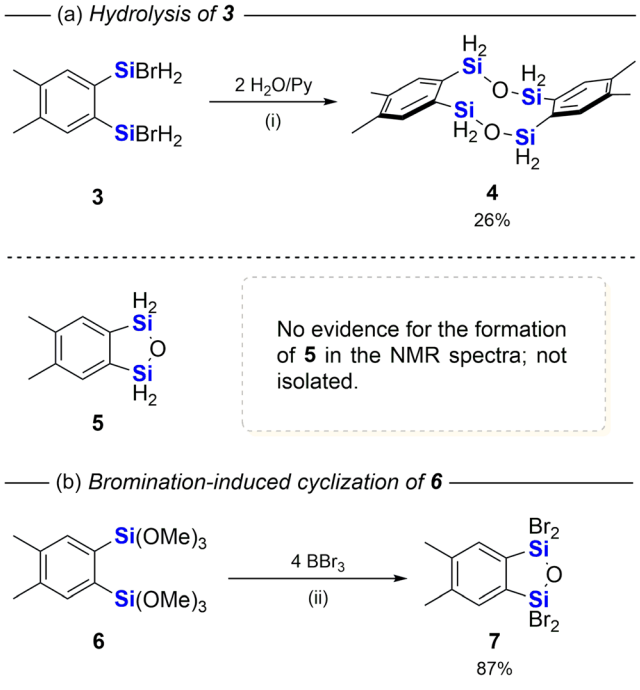

Scheme 4. a) Controlled hydrolysis of **3** in the presence of pyridine (Py) as HBr scavenger affords **4**, and b) bromination-induced cyclization of **6** to furnish **7**. Reagents and conditions: (i) 2 equiv. H_2O, 2 equiv. Py, C_6D_6/CH_3CN, room temperature, 5 min.; (ii) 4.0 equiv. BBr_3, C_6H_6, room temperature, 14 h.

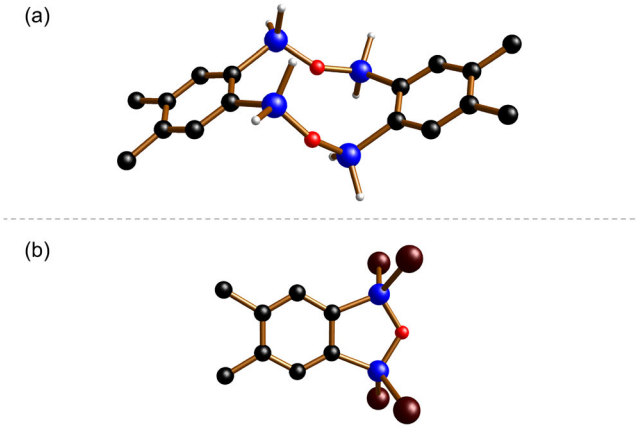

Figure 4. Molecular structures of a) **4** and b) **7** in the crystalline state; C-bonded H atoms omitted for clarity. H: white, C: black, Si: blue, O: red, Br: mahogany.

in the preference of disiloxanes for expanded Si—O—Si′ angles (note, however, that the corresponding bending potential is shallow).[34,35] In compound **4**, these angles measure 152.4(1)° and 146.0(1)°, whereas in compound **7**, the angle is compressed to 114.2(4)°. Mechanistically, the formation of **7** (or **5**) likely involves a cooperative interaction of both Lewis-acidic Si sites with the same MeO (or HO) fragment, which should be less pronounced for hydrogenated than for halogenated silyl groups (generated from **6** via partial MeO/Br exchange).

3. Conclusions

We have developed straightforward synthesis protocols for the complete series of 1,2-bis(trihalogenosilyl)benzenes $\mathbf{1^F}$–$\mathbf{1^I}$. These compounds are subject to significant steric congestion and are currently not accessible by alternative synthetic routes. At the same time, the close proximity of two Lewis-acidic Si centers offers opportunities for novel and potentially valuable reactivity patterns. Systematic variation of the halogen substituents (F, Cl, Br, I) has revealed characteristic trends in key NMR and structural parameters across the series $\mathbf{1^F}$–$\mathbf{1^I}$. Moreover, we have shown that the ditopic Lewis acid $\mathbf{1^F}$ can bind one added F^- ligand in a bridging Si—(μ-F)—Si′ motif and two equivalents of F^- in a mixed bridging/terminal binding mode. Finally, targeted hydrolysis of the 1,2-$(H_2BrSi)_2$-substituted benzene **3** was found to furnish the doubly benzannulated ten-membered $Si_4O_2C_4$ heterocycle **4**, whereas treatment of the 1,2-$((MeO)_3Si)_2$-substituted benzene **6** with BBr_3 affords the 1,3-disila-2-oxaindane **7** with no appreciable formation of its decacyclic dimer. Compound **7**, which is significantly more accessible than its tetrachlorinated congener,[15] represents a versatile monomer for the future synthesis of hybrid organic/inorganic polysiloxanes.

Acknowledgements

The authors gratefully acknowledge Christoph D. Buch for computing the F^--ion affinities. The authors also thank Evonik Operations GmbH, Rheinfelden (Germany), for the generous donation of Si_2Cl_6. Parts of this research (projects I-20220822 and R-20240674) were carried out on the P24 beamline at PETRA III at DESY, a member of the Helmholtz Association (HGF).

Open Access funding enabled and organized by Projekt DEAL.

Conflict of Interest

The authors declare no conflict of interest.

Data Availability Statement

The data that support the findings of this study are available in the supplementary material of this article.

Keywords: cyclization · fluorides · halogenation · Lewis acids · silanes

[1] T. Hiyama, M. Oestreich, *Organosilicon Chemistry*, Wiley-VCH, Weinheim **2019**.
[2] T. J. Barton, P. Boudjouk, *Silicon-Based Polymer Science*, American Chemical Society, Washington D.C. **1989**.
[3] A. D. Dilman, S. L. Ioffe, *Chem. Rev.* **2003**, *103*, 733.
[4] D. Hartmann, M. Schädler, L. Greb, *Chem. Sci.* **2019**, *10*, 7379.
[5] U. Eduok, O. Faye, J. Szpunar, *Prog. Org. Coat.* **2017**, *111*, 124.
[6] M. L. Gringolts, M. V. Bermeshev, K. L. Makovetsky, E. S. Finkelshtein, *Eur. Polym. J.* **2009**, *45*, 2142.
[7] E. S. Finkelshtein, M. L. Gringolts, N. V. Ushakov, V. G. Lakhtin, S. A. Soloviev, Y. P. Yampol'skii, *Polymer* **2003**, *44*, 2843.
[8] V. A. Zhigarev, R. Y. Nikiforov, V. G. Lakhtin, G. A. Shandryuk, N. A. Belov, M. L. Gringolts, *Polymer* **2023**, *273*, 125864.
[9] O. Mukbaniani, M. Matsaberidze, M. Karchkhadze, L. Khananashvili, V. Achelashvili, *J. Appl. Polym. Sci.* **2002**, *84*, 1409.
[10] D. B. Cordes, P. D. Lickiss, F. Rataboul, *Chem. Rev.* **2010**, *110*, 2081.
[11] H. Shi, J. Yang, M. You, Z. Li, C. He, *ACS Mater. Lett.* **2020**, *2*, 296.
[12] A. J. Barry, J. W. Gilkey, D. E. Hook, *Ind. Eng. Chem.* **1959**, *51*, 131.
[13] I. Georg, J. Teichmann, M. Bursch, J. Tillmann, B. Endeward, M. Bolte, H.-W. Lerner, S. Grimme, M. Wagner, *J. Am. Chem. Soc.* **2018**, *140*, 9696.
[14] 1,2-$(Cl_3Si)_2C_6H_4$ was allegedly obtained from 1,2-$Cl_2C_6H_4$ and $HSiCl_3$ at 300 °C upon γ-irradiation: B. I. Vainshtein, L. P. Bogovtseva, *Zh. Obshch. Khim.* **1976**, *46*, 852.
[15] M. Schmidt, J. Gilmer, A. Virovets, M. Bolte, H.-W. Lerner, M. Wagner, *Chem. Eur. J.* **2024**, *30*, e202402998.
[16] The synthesis procedure of this compound is described in the Supporting Information.
[17] The chemical shift values discussed below with reference to literature data were in part recorded in different solvents. Since ^{13}C, ^{19}F, and ^{29}Si NMR chemical shifts are only weakly affected by the choice of solvent, we have omitted this specification for the sake of clarity. Where relevant, solvent information can be found in the Supporting Information or the cited literature.
[18] a) M. G. Voronkov, E. V. Boyarkina, I. A. Gebel', A. I. Albanov, S. V. Basenko, *Russ. J. Gen. Chem.* **2005**, *75*, 1927; b) F. Popp, J. B. Nätscher, J. O. Daiss, C. Burschka, R. Tacke, *Organometallics* **2007**, *26*, 6014.
[19] N. Weidemann, G. Schnakenburg, A. C. Filippou, *Z. Anorg. Allg. Chem.* **2009**, *635*, 253.
[20] In contrast to the ^{29}Si nuclei of our compounds, the ^{13}C nucleus of H_3C–X becomes progressively more shielded as the valence-electron count of X increases, likely due to magnetic anisotropy effects [$\delta(^{13}C) = 71.6$ (X = F), 25.6 (X = Cl), 9.6 (X = Br), −24.0 (X = I)]: K. B. Wiberg, W. E. Pratt, W. F. Bailey, *J. Org. Chem.* **1980**, *45*, 4936.
[21] N. Wiberg, A. F. Holleman, *Lehrbuch der Anorganischen Chemie*, De Gruyter, Berlin **2007**.
[22] J. Mason, *Multinuclear NMR*, Plenum Press, New York **1987**.
[23] Brittain et al. have stated that "For a non-bonded F—F distance (d_{FF}) ≤ 3.20 Å and for fluorines separated by four or more bonds, coupling is mediated primarily by 'TS' coupling." Here, 'TS' stands for 'through-space'; in compound $\mathbf{1^F}$, the shortest d_{FF} between the two SiF_3 groups in the solid-state structure is 2.848(2) Å and the F atoms are separated by five bonds: S. K. Rastogi, R. A. Rogers, J. Shi, C. T. Brown, C. Salinas, K. M. Martin, J. Armitage, C. Dorsey, G. Chun, P. Rinaldi, W. J. Brittain, *Magn. Reson. Chem.* **2016**, *54*, 126.
[24] Compound $\mathbf{1^I}$ crystallizes with two crystallographically independent molecules in the asymmetric unit. Since their key geometric parameters are very similar (Figure S73b), only one of them [containing Si(1)/Si(2); cf. the cif file] is used for the overlay and for comparison with $\mathbf{1^F}$—$\mathbf{1^{Br}}$.
[25] N. W. Mitzel, P. T. Brain, M. A. Hofmann, D. W. H. Rankin, R. Schrock, H. Schmidbaur, *Z. Naturforsch. B* **2002**, *57*, 202.
[26] The average values with standard deviations in square brackets were calculated from the individual geometric parameters provided in the cif file.
[27] For selected publications on F^- ion complexation by (oligodentate) Si-based Lewis acids, see: a) T. Hoshi, M. Takahashi, M. Kira, *Chem. Lett.* **1996**, *25*, 683; b) D. Brondani, F. H. Carré, R. J. P. Corriu, J. J. E. Moreau, M. Wong Chi Man, *Angew. Chem., Int. Ed. Engl.* **1996**, *35*, 324; c) D. Kost, I. Kalikhman, *The Chemistry of Organic Silicon Compounds*, Vol. 2 (Eds.: Z. Rappoport, Y. Apeloig), John Wiley & Sons, Chichester **1998**, pp. 1340–1351; d) M. Kira, E. Kwon, C. Kabuto, K. Sakamoto, *Chem. Lett.* **1999**, *28*, 1183; e) J. Horstmann, M. Niemann, K. Berthold, A. Mix, B. Neumann, H.-G. Stammler, N. W. Mitzel, *Dalton Trans.* **2017**, *46*, 1898; f) J. Gnidovec, E. Gruden, M. Tramšek, J. Iskra, J. Kvíčala, G. Tavčar, *Dalton Trans.* **2023**, *52*, 5085.
[28] K. Tamao, T. Hayashi, Y. Ito, M. Shiro, *Organometallics* **1992**, *11*, 2099.
[29] K. Tamao, T. Hayashi, Y. Ito, M. Shiro, *J. Am. Chem. Soc.* **1990**, *112*, 2422.
[30] The bis(tetrafluorosilicate) $[K(18\text{-crown-6})]_2[F_4SiCH_2CH_2SiF_4]$ devoid of a bridging F^- ligand, was reported: S. E. Johnson, R. O. Day, R. R. Holmes, *Inorg. Chem.* **1989**, *28*, 3182.
[31] The gas-phase F^--ion affinities of $\mathbf{1^F}$ and Tamao's 1,2-$(F_2PhSi)_2C_6H_4$, reported in ref. [28], were calculated to be 327.6 and 314.8 kJ mol^{-1}, respectively. The higher value of $\mathbf{1^F}$ is consistent with the presence of six rather than four electronegative F substituents in the molecule. For F^- affinities of other Si-based Lewis acids, see: P. Erdmann, J. Leitner, J. Schwarz, L. Greb, *ChemPhysChem* **2020**, *21*, 987.
[32] In the ^1H NMR spectrum of the sublimation residue, prominent signals corresponding to compound **4** are still clearly detectable. Given that the sublimed fraction of **4** was already not entirely pure at this stage (Figure S52), we terminated the sublimation process in order to prioritize purity over quantity. It should be noted, however, that the actual conversion to **4** was higher than 26%.

[33] Although the moderate yield of compound **4** (26%) does not allow us to conclusively exclude the formation of some 1,3-disila-2-oxaindane, we could not isolate it or even unequivocally identify it by NMR analysis of the crude hydrolysis product.
[34] S. Grabowsky, M. F. Hesse, C. Paulmann, P. Luger, J. Beckmann, *Inorg. Chem.* **2009**, *48*, 4384.
[35] F. Dankert, C. von Hänisch, *Eur. J. Inorg. Chem.* **2021**, *2021*, 2907.

Manuscript received: July 31, 2025
Revised manuscript received: September 3, 2025
Version of record online: October 24, 2025

